Journal of Solid State Chemistry **165,** 74–78 (2002)
doi:10.1006/jssc.2001.9495, available online at http://www/idealibrary.com on IDEAL®

Preparation, Structure, and Properties of $V_2GeO_4F_2$—Chains of VO_4F_2 Octahedra in the First V(III) Metallate Fluoride

S. N. Achary,* A. K. Tyagi,* and J. Köhler†,[1]

*Applied Chemistry Division, Bhabha Atomic Research Center, Mumbai 400 085, India; and †Max-Planck-Insitut für Festkörperforschung Heisenbergstrasse 1, D-70569 Stuttgart, Germany
E-mail: j.koehler@fkf.mpg.de

Received August 17, 2001; in revised form November 23, 2001; accepted December 21, 2001

Powder samples of the new oxide fluoride $V_2GeO_4F_2$ have been obtained by the reaction of appropriate amounts V_2O_3, VF_3, and GeO_2 at 700°C for 18 h in an argon-filled sealed platinum tube. $V_2GeO_4F_2$ crystallizes in the space group *Pnma* with $a = 9.336(1)$, $b = 8.898$ (1), and $c = 4.912$ (1) Å. The structure has been refined from X-ray powder diffraction data using the Rietveld method ($R_{int} = 5.5\%$ and $R_p = 9.8\%$). The structure of $V_2GeO_4F_2$ exhibits close packed layers of the anions with an ordering of O and F. The characteristic building units are discrete GeO_4 tetrahedra with Ge–O distances of 1.75–1.80 Å. The V are coordinated by four O and two F to form VO_4F_2 octahedra connected via two common edges to give zigzag chains. These chains are linked via corners to form a three-dimensional network. The temperature dependence of the magnetic susceptibility of $V_2GeO_4F_2$ indicates antiferromagnetic correlations. © 2002 Elsevier Science (USA)

Key Words: **vanadium oxide fluoride; crystal structure; magnetic properties.**

INTRODUCTION

Low-valent V(III) oxides have attracted considerable interest since they often exhibit unusual physical properties. For example, the binary oxide V_2O_3 (1) undergoes a transition from its metallic state to an insulating antiferromagnetic state at 155 K, accompanied by a structural phase transition. Such many body phenomena, which are called Mott transitions (2), are also found in some ternary V(III) oxides, e.g., $LaVO_3$, which shows anomalous diamagnetic behavior below 133 K (3–5). The V–Ge–O system has been repeatedly studied by phase analyses on the basis of XRD powder data (6, 7). Most of the characterized phases are mixed valent V(III,IV) oxides and only one V(III) germanate, V_2GeO_5, has been found so far (8). However, only *d* values without any further structural information are given for this phase. During our recent studies of the V_2O_3–GeO_2 system, we found that the structure of the phase V_2GeO_5 seems to be related to the mineral topaz $Al_2SiO_4F_2$ (9, 10) and can be described as V_2GeO_{6-x} ($x \approx 1.0$) in which one oxygen position is only 50% occupied. Because of twinning and disorder in crystals of this compound, we have encountered considerable difficulties in structure refinements. In order to synthesize a filled isoelectronic analogue that exhibits no phase width, it seemed promising to search for a hitherto unknown oxide fluoride with the composition $V_2GeO_4F_2$, which may be expected to exhibit full occupancies of the anion sites. The anticipated compound could be prepared as dark green powder samples and the structure could be refined using the Rietveld method on the basis of powder X-ray data.

EXPERIMENTAL

The title compound was synthesized from a mixture of an appropriate molar ratio of GeO_2, V_2O_3, and VF_3 (Alfa, 99.9%), which was intimately ground in an argon-filled glove box and pressed into a pellet. The pellet was placed in a platinum tube that was sealed and then transferred to a argon-filled quartz glass ampoule. Homogeneous powder samples of $V_2GeO_4F_2$ were obtained by heating this mixture at 700°C for 18 h followed by a cooling to room temperature by switching off the furnace. They are dark green and stable in air and do not decompose under water after hours.

X-ray powder diffraction (XRD) data for the Rietveld refinement were collected on a STOE STADI-P powder diffractometer equipped with a mini-PSD detector, with a rotating sample in symmetric transmission mode (germanium monochromator, Cu$K\alpha_1$ radiation). For $V_2GeO_4F_2$, the data were refined by the full powder profile method using the CSD software (11). Atomic parameters from the

[1]To whom correspondence should be addressed.

0022-4596/02 $35.00

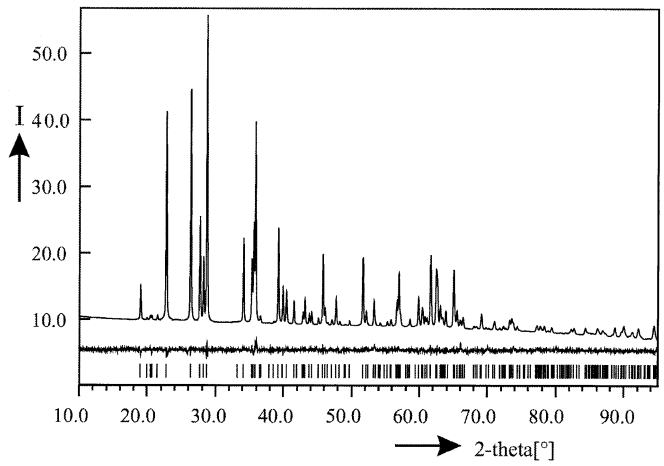

FIG. 1. Rietveld refinement of the crystal structure $V_2GeO_4F_2$. Observed diffraction pattern (upper curve) and difference between calculated and observed intensities (lower curve).

mineral topaz were used as starting parameters and initial atomic coordinates were refined followed by the refinement of thermal parameters of the cations. The thermal parameters of the anions were fixed to 1.0. The profile parameters, background scale, zero-shift, and asymmetry parameter were also refined using a pseudo-Voigt function. The profile refinement of this phase shows a good agreement with that observed as indicated by $R_{\text{int}} = 5.5\%$ and $R_p = 9.8\%$, see Fig. 1. The details of the final Rietveld refinement, which have been performed with a certain anion ordering of O and F as found in topaz, are given in Table 1. The atomic parameters are listed in Table 2 and interatomic distances in Table 3.

RESULTS AND DISCUSSION

The structure of $V_2GeO_4F_2$ is shown in Fig. 2. It can be described in terms of a close packing of layers of O(1) and F (type α) and O(2) and O(3) (type β), which are stacked along [100] according to the motif $A(\alpha)B(\beta)A(\alpha)C(\beta)$, etc., of chc. One-third of the octahedral holes are occupied by V and one-twelfth of the tetrahedral holes by Ge. The occurrence of this structure type is so far limited to a handful of oxide fluorides or oxide hydroxides, such as the mineral topaz $Al_2SiO_4F_2$ (9, 10) or the high-pressure form of dialuminum dihydroxo-tetraoxogermanate, $Al_2GeO_4(OH)_2$ (12, 13). It is worth mentioning that there is also a stacking variant, the low-pressure form of $Al_2GeO_4(OH)_2$ (14), which exhibits a cubic close-packing (*ABC*, etc.) of O and O_H atoms.

Motifs of the mutual adjunction (15) together with bond order sums (16) for $V_2GeO_4F_2$ are given in Table 4. According to $V_2GeO(1)O(2)O(3)_2F_2$ the structure contains four crystallographically different positions for the anions, and the assumed underlying anion ordering as in topaz is confirmed by the calculated bond order sums of $\sum S_i \approx 1.0$ for the F and $\sum S_i \approx 2.00$–2.08 for the O. This is in contrast to the situation found for many other oxide fluorides, in which a random arrangement of O and F in the anion positions is found. However, the distances within the GeO_4 tetrahedra lie between 1.75 and 1.8 Å, similar to those found in other *ortho*-germanates, e.g., Li_4GeO_4 (17), $Ag_4(GeO_4)$ (18), or the recently discovered oxide fluoride $NaCa_2GeO_4F$ (19), see Table 3. Comparable Ge–F distances are found in fluorides containing sixfold coordinated Ge, e.g., 6×1.78 Å in Na_2GeF_6 (20), but in GeF_4 (21), the only compound in which Ge is tetrahedrally coordinated by F, the Ge–F distances are much shorter, i.e., 1.66 Å. It appears also reasonable from this to assume in $V_2GeO_4F_2$ an order of O and F in such a way that only

TABLE 1
Powder Crystallographic Data, Experimental Conditions, and Rietveld Data for $V_2GeO_4F_2$[a]

Name	Vanadium (III) difluorogermanate (IV)
Formula	$V_2GeO_4F_2$
Formula weight [g/mol]	276.5
Space group, Nr.	*Pnma*, 62
Lattice constants (Å)	$a = 9.336(1)$, $b = 8.898(1)$, $c = 4.912(1)$
Cell volume (Å^3)	408.05(2)
$F(000)$ (electrons)	512
Number of atoms in cell	36
Calculated density (g/cm^3)	4.50(1)
Absorption coefficient (Cm^{-1})	497.82
Radiation and wavelength	Cu$K\alpha_1$, 1.54051 Å
Diffractometer	Powder
Mode of refinement	Full profile
Number of atom sites	6
Number of free parameters	22
2Δ and $\sin\theta/\lambda$ (max)	96.4, 0.484
Reflections used in refinement	45
R_{Int}, R_P	0.0545, 0.0979
Goodness-of-fit	0.300
Scale factor	1.79(2)

[a]Further details of the crystal structure investigation may be obtained from the Fachinformationzentrum Energie, Physik, Mathematik, D-76344 Eggenstein-Leopoldshafen 2, upon quoting the depository number CSD-412050, the name of the authors, and the journal citation.

TABLE 2
Atomic Coordinates and Equivalent Isotropic Displacement Parameters (Å$^2 \times 10^4$) for $V_2GeO_4F_2$

Atom	Position	x/a	y/b	z/c	B (is/eq)
Ge	4*c*	0.4415(2)	$\frac{1}{4}$	0.3980(4)	0.76(4)
V	8*d*	0.1334(1)	0.0829(2)	0.6011(4)	0.52(4)
F	8*d*	0.7492(4)	0.0598(4)	0.5923(9)	1.0[a]
O1	4*c*	0.2507(8)	$\frac{1}{4}$	0.4505(13)	1.0[a]
O2	4*c*	0.0293(7)	$\frac{1}{4}$	0.7870(12)	1.0[a]
O3	8*d*	0.9960(4)	0.0880(5)	0.2901(9)	1.0[a]

[a]Fixed during refinement.

TABLE 3
Selected Interatomic Distances (Å) with Standard Deviations in $V_2GeO_4F_2$

Ge–O2	1.752(1)
O3	1.787(1) × 2
O1	1.799(1)
V–F	1.864(2)
F	1.928(1)
O1	1.990(2)
O3	1.996(2)
O2	1.998(2)
O3	2.014(1)

TABLE 4
Motifs of Mutual Adjunction (15), Coordination Numbers (CN), and Bond Order Sums [a] ($\sum s_i$) (16) for $V_2GeO_4F_2$

Atoms	O1	O2	2 O3	2 F	CN	$\sum s_i$
Ge	1/1	1/1	2/1	—	4	3.99
2 V	1/2	1/2	2/2	2/2	6	3.00
CN	3	3	3	2		
$\sum s_i$	1.97	2.08	1.97	1.00		

[a] $\sum s_i = \sum \exp[(r_o - r_i)]$ ($B = 0.37$ Å) with r_o values Ge–O = 1.780 Å, V–O = 1.743 Å, and V–F = 1.638 Å.

Ge is coordinated by O. The bond order sums of $\sum S_i \approx 3.00$ for V and $\sum S_i \approx 4.0$ for Ge clearly reflect that Ge has the oxidation state 4+ and V the oxidation state 3+, and $V_2GeO_4F_2$ can be well described as a V(III) *ortho*-germanate (IV) fluoride.

The V are octahedrally coordinated by four O and two F with cation fluorine bond lengths slightly shorter ($d_{V-F} = 1.86$ and 1.92 Å) than the cation oxygen bond lengths ($d_{V-O} = 1.99$–2.01 Å). This could have been expected from Shannon's ionic radii (22), but it seems also reasonable due to the fact that the F are coordinated by two V and the O by two V and one Ge. The VO_4F_2 octahedra are connected via common O(1)–O(2) and O(3)–O(3) edges to zigzag chains of the composition $VO_{4/2}F_{2/1} = VO_2F_2$, see Fig. 3. The distances within the VO_4F_2 octahedra are given together with the corresponding connectivity with neighboring polyhedra by the Schlegel diagrams and Schlegel projections (23) in Fig. 4. It is evident from Fig. 4b that the VO_2F_2 octahedra within one chain are only connected via common corners with GeO_4 tetrahedra and VO_4F_2 octahedra of neighboring chains to form a three-dimensional network, see Fig. 2. The common edges are formed only by O, whereas the F occupy the remaining two positions, as one would have expected from electrostatic reasons are similar to what has been found in other oxide fluorides, e.g., $Sn_4O_2F_{10}$ (24). The V–V distances are 2.97 Å across the O(1)–O(2) edge and 3.06 Å across the O(3)–O(3) edge. This contrasts the situation found for the low-temperature modification V_2O_3 in which short distances of 2.86–2.73 Å across the edges of the VO_6 octahedra with direct metal–metal bonded V are found. The absence of direct V–V bonding in $V_2GeO_4F_2$ is also indicated by the short distances of the common O–O edges, which are 2.65 Å for O(1)–O(2) and 2.59 Å for O(1)–O(2). Obviously in $V_2GeO_4F_2$ the off-center position of V in combination with the formation of direct metal–metal bonds is less favorable than that of V_2O_3.

For an electrostatic analysis and a check of the assumed order of O and F we have calculated MAPLE (25) (Madelung Part of Lattice Energy) for $V_2GeO_4F_2$ for different charge distributions within the anion sublattice, see Table 5. Usually, in highly ionic compounds the calculated MAPLE value of a ternary of multinary compound, in this case $V_2GeO_4F_2$, should not deviate by more than 1% from the corresponding sum of the MAPLE values of the binary compounds, here V_2O_3 (26), VF_3 (27), and GeO_2 (28), respectively.

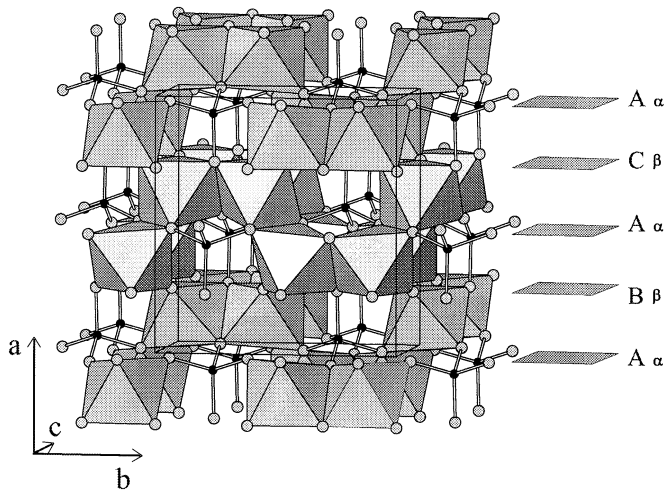

FIG. 2. Projection of the crystal structure of $V_2GeO_4F_2$. Small black circles represent Ge, large gray circles F. VO_4F_2 octahedra and GeO_4 tetrahedra and graphically emphasized, and the stacking sequence of the layers O(1)–F(α) and O(2) –O(3) (β) is given.

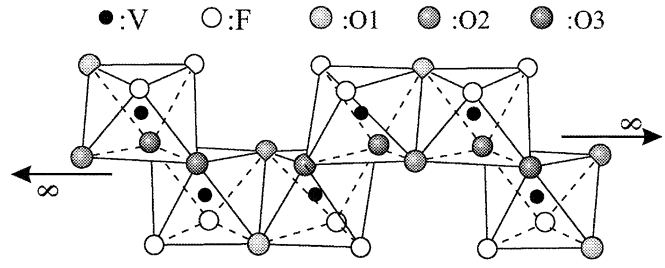

FIG. 3. Projection of a zigzag chain of edge-sharing VO_4F_2 octahedra in $V_2GeO_4F_2$.

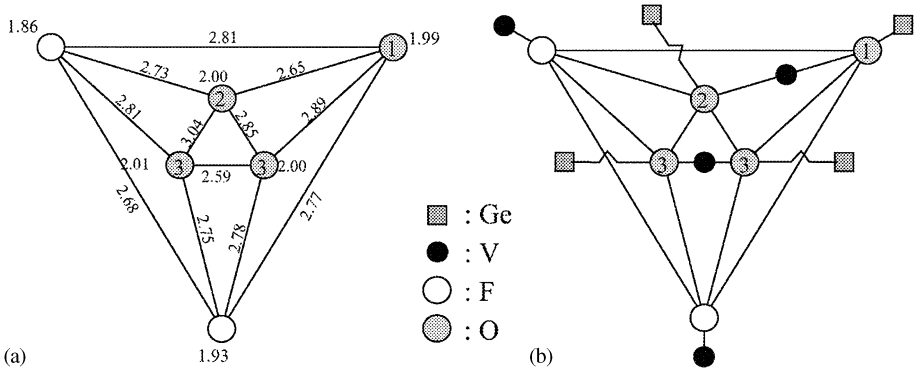

FIG. 4. Schlegel projections and Schlegel diagrams (23) of a VO_4F_2 octahedron (a and b) in $V_2GeO_4F_2$. In (a) the V–F and V–O distances (Å) are given at the terminal positions. The O–F and O–O distances with respect to the central atom (not included) are indicated next to the edges. Vertex-sharing and edge-sharing with VO_4F_2 octahedra and GeO_4 tetrahedra are given in (b)

According to

$$2 \times \mathrm{MAPLE}(V_2O_3) + 2 \times \mathrm{MAPLE}(VF_3) + 3 \times \mathrm{MAPLE}(GeO_2) = 3 \times \mathrm{MAPLE}_{\mathrm{bin}}.(V_2GeO_4F_2)$$
$$2 \times 4121.0 + 2 \times 1528.4 + 3 \times 3358.5 = 3 \times 7120.8 \text{ kcal/mol},$$

the sum of MAPLE values for the binary components is only 0.1% smaller for the charge distribution, see Table 5, than the calculated value of 7127.1 kcal/mol for $V_2GeO_4F_2$ and is in good agreement with the structure refinement, especially with respect to assumed order of O and F within the anion sublattice. Structural models with O and F positions and the other way around always result in values with deviations from $\mathrm{MAPLE}_{\mathrm{bin}}.(V_2GeO_4F_2)$ larger than 5%, indicating that it does not seem reasonable to assume an anion order other than the given one.

Measurements of the electrical conductivity at room temperature show that $V_2GeO_4F_2$ is an insulator with an electrical resistivity higher than $10^6\,\Omega$/cm. The question arises whether $V_2GeO_4F_2$ undergoes a phase transition at higher temperatures to a metallic state as observed for V_2O_3. The magnetic susceptibility of a sample of $V_2GeO_4F_2$ was measured using a MPMS Quantum Design SQUID at a constant external magnetic field of 0.01 T as a function of temperature. The corresponding data of the magnetic susceptibility and the effective magnetic moment vs temperature for $V_2GeO_4F_2$ are given in the Figs. 5a and 5b, respectively. Obviously $V_2GeO_4F_2$ does not show classical Curie–Weiss behavior and the magnetic moment at room temperature corresponds to approximately $2.5\,\mu_B$. This is far below the expected value of $4.0\,\mu_B$, which is calculated according to

$$\mu_{\mathrm{eff}} = g\sqrt{s(s+1)\cdot n},$$

with $g = 2.0$, $s = 1$ (d^2 ion), and $n = 2$ (number of V atoms per formula unit). Obviously there is a significant compensation of moments due to antiferromagnetic exchange interactions, which are also indicated by the broad shoulder between 100 and 200 K, see insert in Fig. 5a. The strong increase below 50 K is attributed to a small amount of paramagnetic impurities, which cannot be detected in the X-ray powder diffraction diagram. As the structure of $V_2GeO_4F_2$ contains chains of edge-sharing VO_4F_2 octahedra connected only via F to a three-dimensional network, see Fig. 4, one can expect $V_2GeO_4F_2$ to be a candidate for the study of 1D magnetic exchange of V^{3+}.

CONCLUSION

We have synthesized the new oxide fluroide $V_2GeO_4F_2$ that has been characterized by X-ray powder diffraction

TABLE 5
Contribution of the Atoms to the Madelung Part of the Lattice Energy (MAPLE) (kcal/mol) (25) for Models of $V_2GeO_4F_2$ (a)–(d) with Different Charge Distributions

Atom	(a)	MAPLE	(b)	MAPLE	(c)	MAPLE	(d)	MAPLE
2 V	+3.0	2×1196.67	+3	2×1203.84	+3	2×1205.94	+3	2×1180.25
Ge	+4.0	1904.46	+4	1842.17	+4	1835.41	+4	2035.84
2 F	−1.667	2×334.31	−2	2×451.32	−2	2×456.48	−1	2×147.86
O1	−1.667	456.26	−2	591.90	−2	217.10	−2	616.43
O2	−1.667	474.12	−2	635.31	−1	228.85	−2	613.84
2 O3	−1.667	2×459.57	−1	2×223.02	−2	2×606.03	−2	2×602.40
		$\sum = 6815.96$		$\sum = 6825.74$		$\sum = 6818.25$		$\sum = 7127.13$

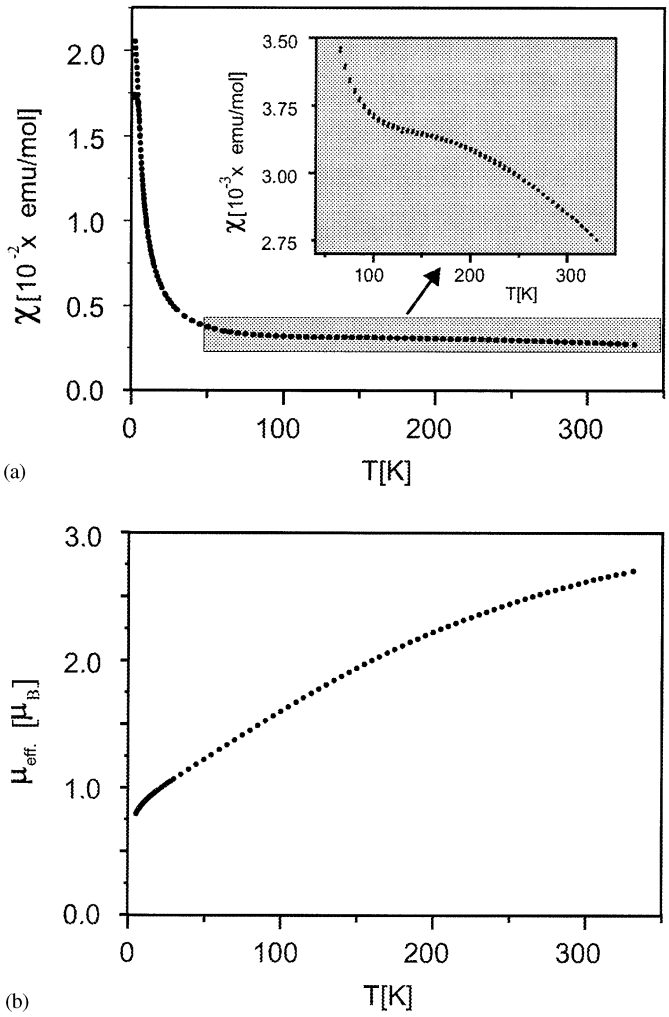

FIG. 5. Temperature dependence of (a) the magnetic susceptibility vs temperature for $V_2GeO_4F_2$ and (b) the calculated magnetic moment of $V_2GeO_4F_2$.

and measurements of the magnetic susceptibility. Strong magnetic correlations indicate that there are 1D interactions of V^{3+} along chains of edge-sharing VO_4F_2 octahedra. In order to study the exchange of d^1 ions in similar chains it seems promising to replace V^{3+} with Ti^{3+}. We have further succeeded in preparing such oxide fluorides, e.g., $VTiGeO_4F_2$ and $Ti_2GeO_4F_2$, on which we will report soon.

ACKNOWLEDGMENTS

We thank professor Dr. A. Simon for his support of this work and Dr. R. K. Kremer for helpful discussions. Ms. E. Brücher is thanked for collecting the magnetic data. The authors are grateful to BMBF, Bonn, Germany for financial support of this work.

REFERENCES

1. J. W. Taylor, T. J. Smith, K. H. Andersen, H. Capellmann, R. K. Kremer, A. Simon, O. Schaerpf, K.-U. Neumann, and K. R. A. Ziebeck, *Eur. Phys. J. B* **199,** 207 (1999).
2. N. F. Mott, *Proc. Phys. Soc. A* **62,** 416 (1949).
3. A. V. Mahajan, D. C. Johnston, D. R. Torgeson, and F. Borsa, *Physica C* **185,** 1195 (1991).
4. N. Shirakawa and M. Ishikawa, *Jpn. J. Appl. Phys.* **30,** 755 (1991).
5. A. V. Mahajan, D. C. Johnston, D. R. Torgeson, and F. Borsa, *Phys. Rev. B* **46,** 10,996. (1991).
6. B. Bodiot, C. R. Seances, *Acad. Sci., Ser. C* **296,** 395 (1969).
7. B. Cros, H. Kerner, A. Caramel, and G. Tourne, *C. R. Seances Acad. Sci., Ser. C* **284,** 529 (1977).
8. B. Cros, A. Caramel, and H. Kerner-Czeskleba, *Rev. Chim. Miner.* **14,** 563 (1977).
9. P. H. Ribbe and G. V. Gibbs, *Am. Mineral*, **56,** 24 (1971).
10. Yu. V. Ivanov, E. L. Belokoneva, J. Protas, N. K. Hansen, and V. G. Tsirelson, *Acta Crystallogr. Sect. B* **54,** 774 (1998).
11. L. G. Akselrud, Y. N. Grin, P. Y. Zavalij, V. K. Pecharsky, and V. S. Fundamenskii, *in* "12th European Crystallographic Meeting Abstract of Papers," Moscow, Vol. 3, p. 155, 1989. (Available at http://materials.binghampton.edu/zavalij/.)
12. B. Marler and B. Wunder, *Z. Kristallogr.* **213,** 3 (1998).
13. B. Marler and B. Wunder, *Eur. J. Miner.* **9,** 1147 (1997).
14. C. L. Lengauer, E. Tillmanns, J. Zemann, and J.-L. Robert, *Z. Kristallogr.* **210,** 656 (1995).
15. R. Hoppe, *Angew. Chem.* **92,** 106 (1980); *Angew. Chem. Int. Ed.* **19,** 10 (1980).
16. I. D. Brown and D. Altermatt, *Acta Crystallogr. Sect. B* **41,** 244 (1985).
17. R. Hofmann and R. Hoppe, *Z. Anorg. Allg. Chem.* **555,** 118 (1987).
18. C. Linke, R. Hundt, and M. Jansen, *Z. Kristallogr.* **210,** 850 (1995).
19. L. F. Schneemeyer, L. Guterman, T. Siegrist, and G. R. Kowach, *J. Solid State Chem.* **160,** 33 (2001).
20. F. Averdunk and R. Hoppe, *Z. Anorg. Allg. Chem.* **582,** 111 (1990).
21. J. Köhler, A. Simon, and R. Hoppe, *J. Less-Common Met.* **137,** 333 (1988).
22. R. D. Shannon, and C. T. Prewitt, *Acta Crystallogr. Sect. B* **35,** 745 (1969).
23. R. Hoppe and J. Köhler, *Z. Kristallogr.* **183,** 77 (1988).
24. J.-H. Chang and J. Köhler, *Z. Kristallogr.* **214,** 147 (1999).
25. R. Hoppe, *Angew. Chem.* **78,** 52 (1966); *Angew. Chem. Int. Ed. Eng.* **5,** 95 (1966).
26. M. G. Vincent and K. Yvon, *Acta Crystallogr. Sect. A* **36,** 808 (1980).
27. P. Daniel, A. Bulou, M. Leblanc, M. Rousseau, and J. Nouet, *Mater. Res. Bull.* **25,** 413 (1990).
28. G. S. Smith and P. B. Isaacs, *Acta Crystallogr. Sect. A* **17,** 842 (1964).